Emittance Exchange using thick Bent Solenoid elements

R.C. Fernow
BNL

Exchange Workshop
BNL
11 September 2000

Outline

1. Bent solenoid dynamics
2. Exchange design with rf
3. Specific design

Emittance exchange

Methods of incorporating emittance exchange (EMEX) in cooling lattices

- standalone EMEX sections
- thin dispersive elements periodically in transverse cooling lattice
- conductor-absorber configuration for simultaneous transverse cooling plus EMEX

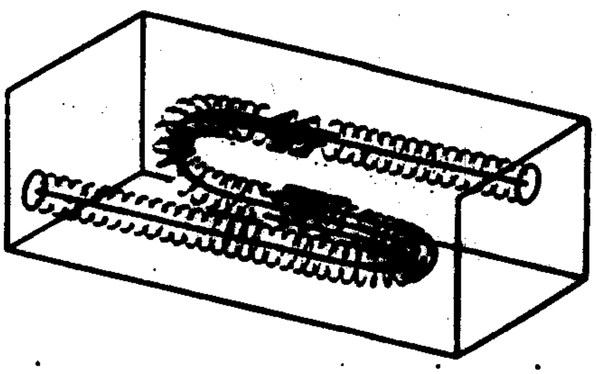

Palmer

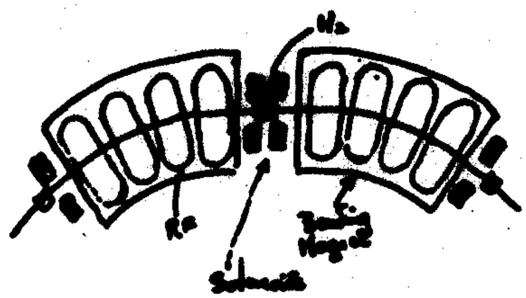

Palmer

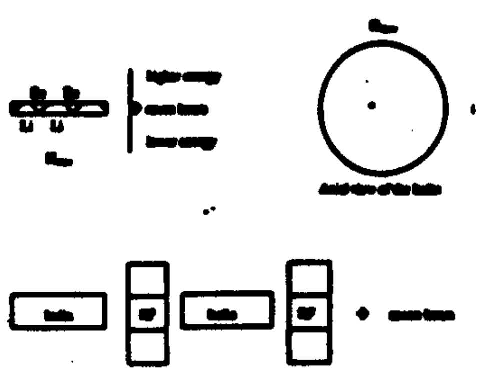

Skrinsky

This study

This study examines

- standalone configuration
- thick bent solenoid elements

Goals for standalone EMEX system

1. the momentum spread should be reduced by a factor of ~0.5
2. the bunch length should approximately equal that of the input beam
3. the transverse area should be symmetric and larger by a factor ~2
4. the transverse divergences should approximately equal that of the input beam
5. the mean momentum should approximately equal that of the input beam

Methods to describe bent solenoid fields

- sum of individual current loops
- analytic fields (ICOOL)
  - 1st order
  - 2nd order

ERROR: typecheck
OFFENDING COMMAND: CSshow

STACK:

1495
(f)

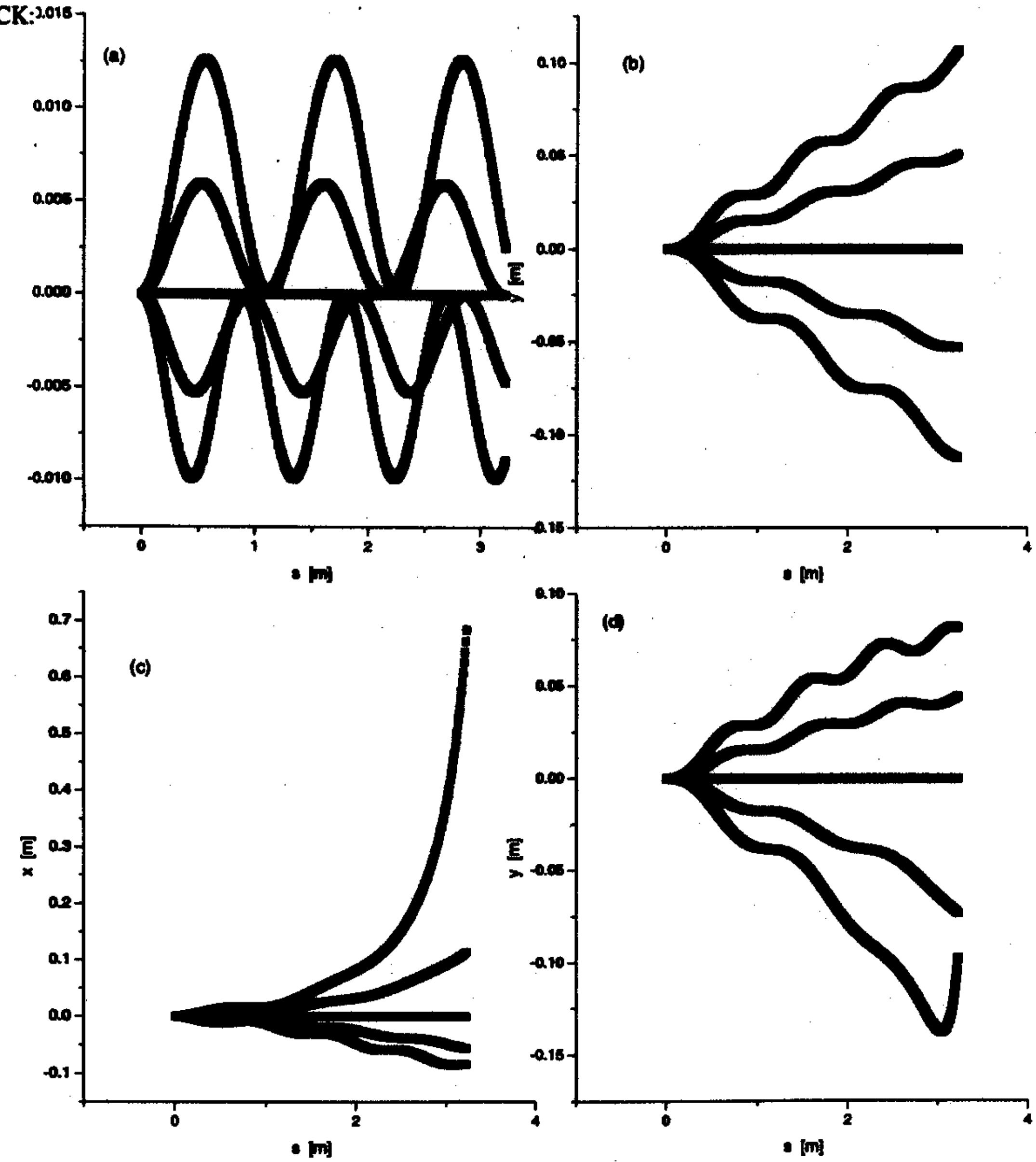

Figure 1. Particle orbits inside the bent solenoid field

1 st order

ERROR: typecheck
OFFENDING COMMAND: CSshow

$L = 1 \lambda_L$

STACK:

1472
(e)

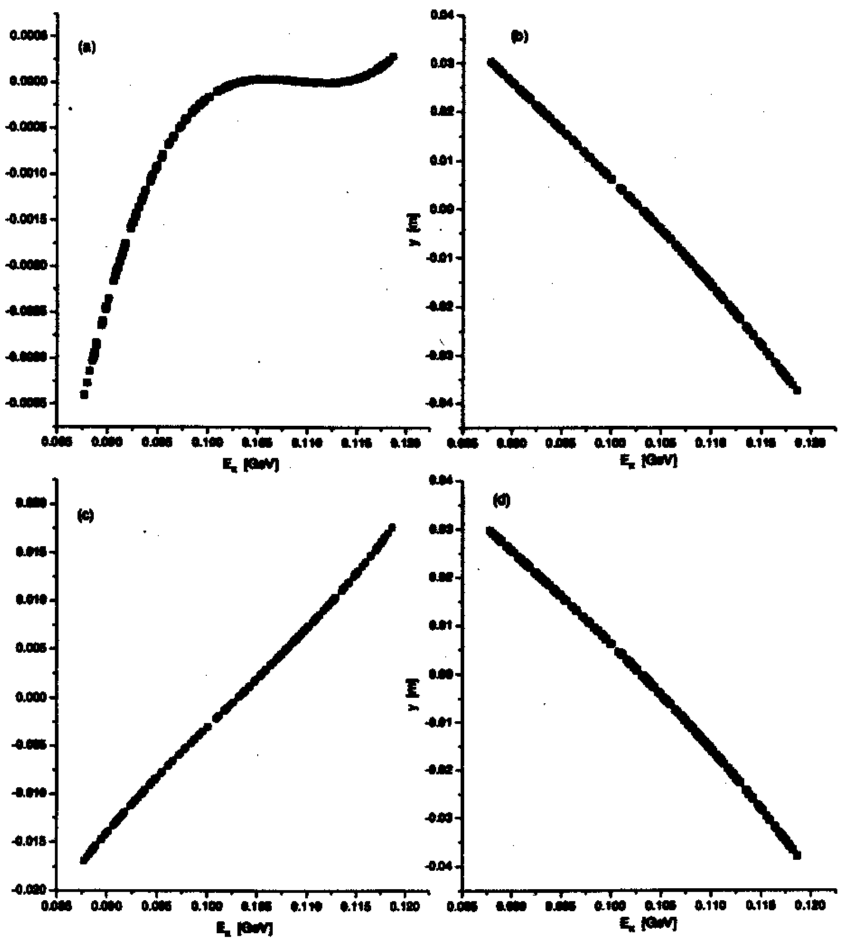

Figure 2. Dispersion for particles uniformly distribut

$L = 1\ \lambda_L$

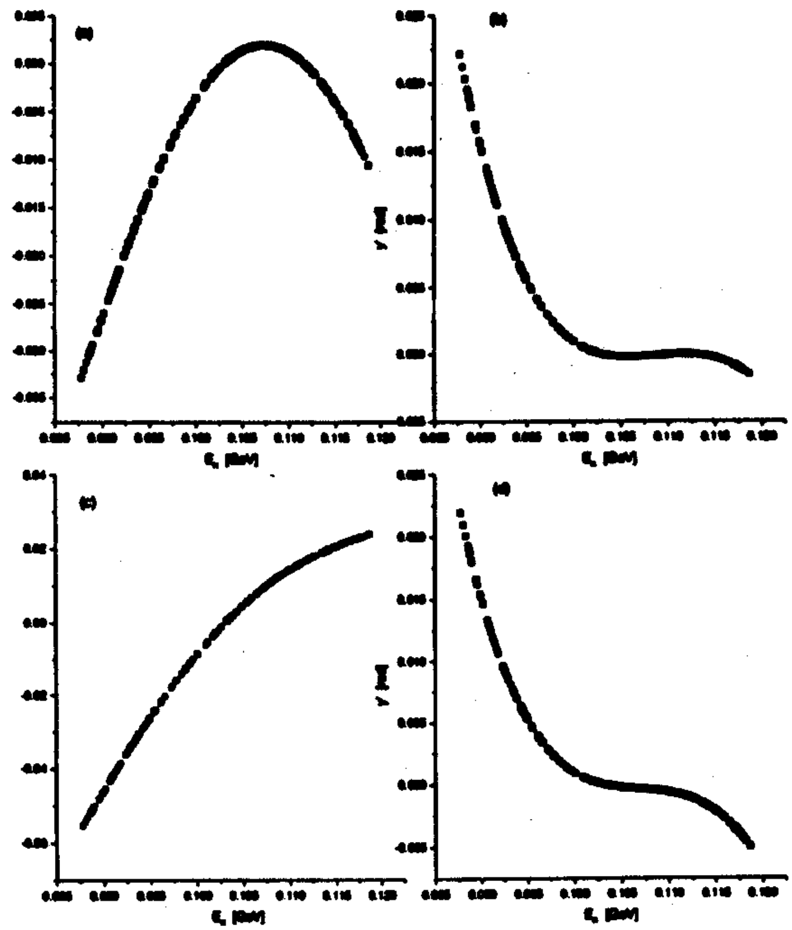

Figure 3. Angular dispersion for particles uniformly distributed between 162 and 198 MeV/c. (a) x' dispersion for uniform dipole field; (b) y' dispersion for uniform dipole field; (c) x' dispersion for field with quad component; (d) y' dispersion for field with quad component.

4 Emittance exchange system design

We now consider the design of an actual emittance exchange system. The first half, dealing with dispersion in y, is shown schematically in Fig. 5.

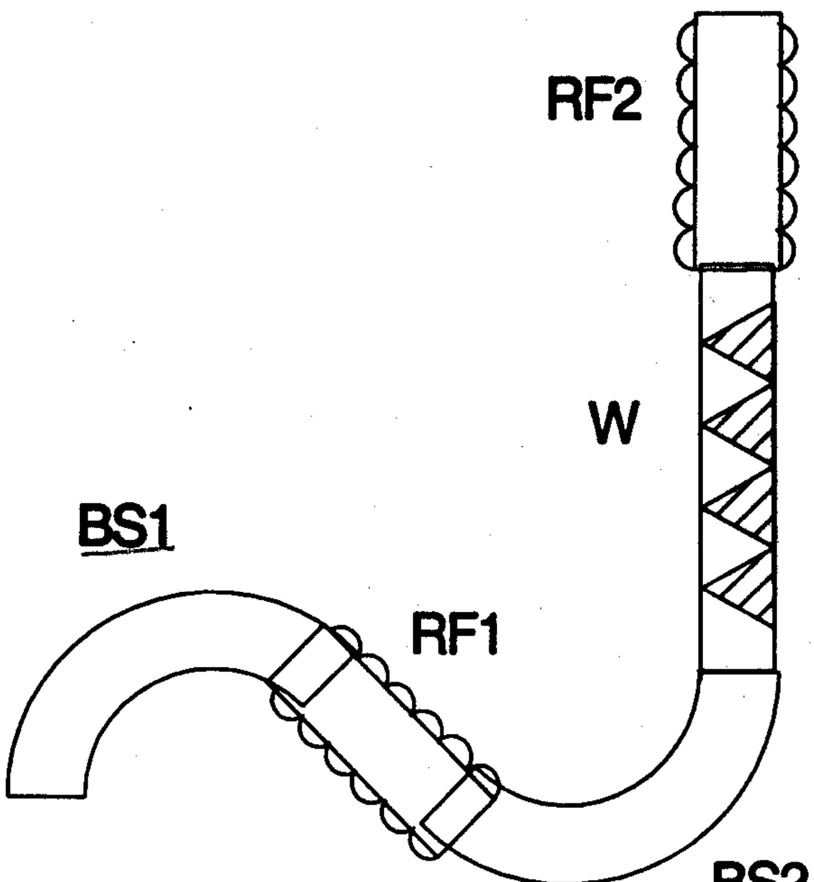

Figure 5. Schematic layout of one half of an emittance exchange system.

configuration

P_z vs t

Bent solenoid fields

- vector potential [Wang & Chao; Morozov & Solov'ev]

$$\vec{A}(x,y,s) = -\frac{1}{2} B_{so}(s) \frac{y}{(1 + h(s)\,x)}\,\hat{x} + \frac{1}{2\,h(s)} B_{so}(s)\,\ln(1 + h(s)\,x)\,\hat{y}$$

- field components

$$\vec{B} = \nabla \times \vec{A}$$

- second order magnetic field components

$$B_x(x,y,s) = -\frac{1}{2}\left(B'_{so}(s)\,x - \frac{1}{2} B_{so}(s)\,h'(s)\,x^2 - \frac{3}{2} B'_{so}(s)\,h(s)\,x^2 \right)$$

$$B_y(x,y,s) = -\frac{1}{2}\left(B'_{so}(s)\,y - 2\,B'_{so}(s)\,h(s)\,xy - B_{so}(s)\,h'(s)\,xy \right)$$

$$B_s(x,y,s) = (1 - h(s)\,x + h(s)^2\,x^2)\,B_{so}(s)$$

- independent solenoid field component

$$B_{so}(s) = B_S\,\Delta\tanh(s;c,e,\lambda)$$

- h(s) is the geometrical curvature

- assume $\rho_{geometry} = \rho_{dipole}$

Dipole field (second order)

$$B_x(x,y,s) = a_{11}(s)\,y + a_{12}(s)\,xy$$
$$B_y(x,y,s) = a_{10}(s) + a_{11}(s)x + \frac{1}{2}a_{12}(s)x^2 + \frac{1}{2}a_{30}(s)y^2$$
$$B_s(x,y,s) = a_{10}'(s)\,y + (a_{11}'(s) - h(s)\,a_{10}'(s))\,xy$$

- independent dipole and quadrupole components

$$a_{10}(s) = B_D\ \Delta\tanh(s;c_1,e_1,\lambda_1)$$
$$a_{11}(s) = B_Q\ \Delta\tanh(s;c_2,e_2,\lambda_2)$$

- sextupole constraints

$$a_{12}(s) = 2\,a_{10}''(s) + a_{10}'(s)\frac{h'(s)}{h(s)} + a_{11}(s)\,h(s) - \frac{1}{h(s)}a_{11}''(s)$$
$$a_{30}(s) = -a_{12}(s) - a_{11}(s)\,h(s) - a_{10}''(s)$$

- curvature

$$h(s) = \frac{q}{p_o}\,B_Y(0,0,s)$$

- satisfies Maxwell's equations to second order

$$\nabla\bullet\vec{B} = 0$$
$$\nabla\times\vec{B} \approx 0$$

(error in a_{12}')

Table 2a Beam parameters		
	Entrance	
p_o	180	MeV/c
σ_X	21.1	mm
σ_Y	21.2	mm
σ_Z	20	mm
σ_{Px}	14.9	MeV/c
σ_{Py}	15.6	MeV/c
σ_{PZ}	9.2	MeV/c
ε_{TN}	2.08	mm
ε_{LN}	1.68	mm
ε_{6N}	7.1	mm^3

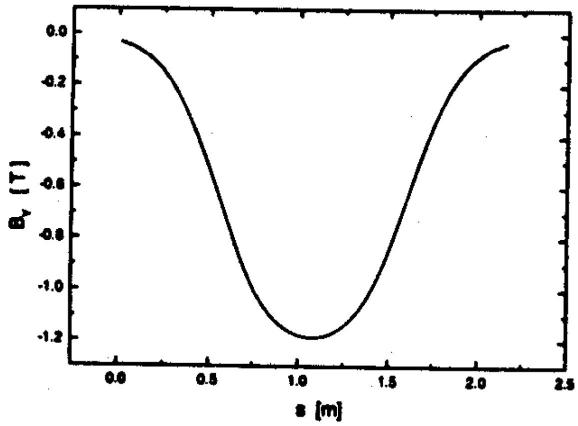

Figure 6. Dipole field profile for BS1. = − BS2

Table 3 Bent solenoid parameters		
B_S	3.5	T
B_D (peak)	±1.19	T
g_Q	0.	T / m
L	2.16	m
θ	143	deg
ρ	0.5	m
c_D	1.06	m
e_D	0.55	m
λ_D	0.3	m

At end of BS2

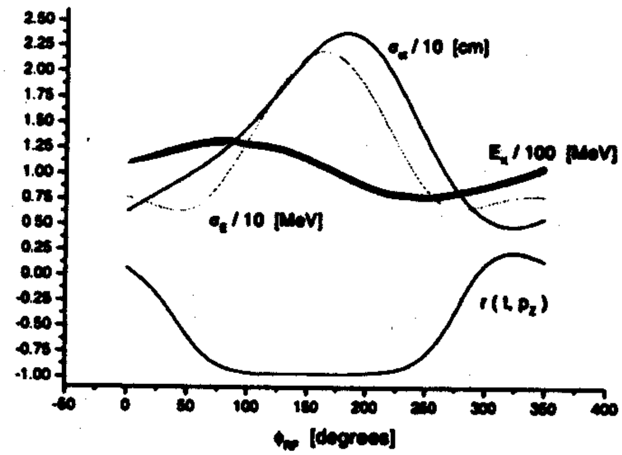

Figure 7. Dependence of average kinetic energy, energy spread, bunch length, and longitudinal phase space correlation on phase for RF1. The gradient is 17 MV/m.

Table 4 RF system design parameter			
RF1	f	400	MHz
	G	17	MV / m
	φ	-14	deg
	N_{cells}	13	
	L_{cell}	16.62	cm
RF2	f	400	MHz
	G	12	MV / m
	φ	24	deg
	N_{cells}	13	
	L_{cell}	16.62	cm

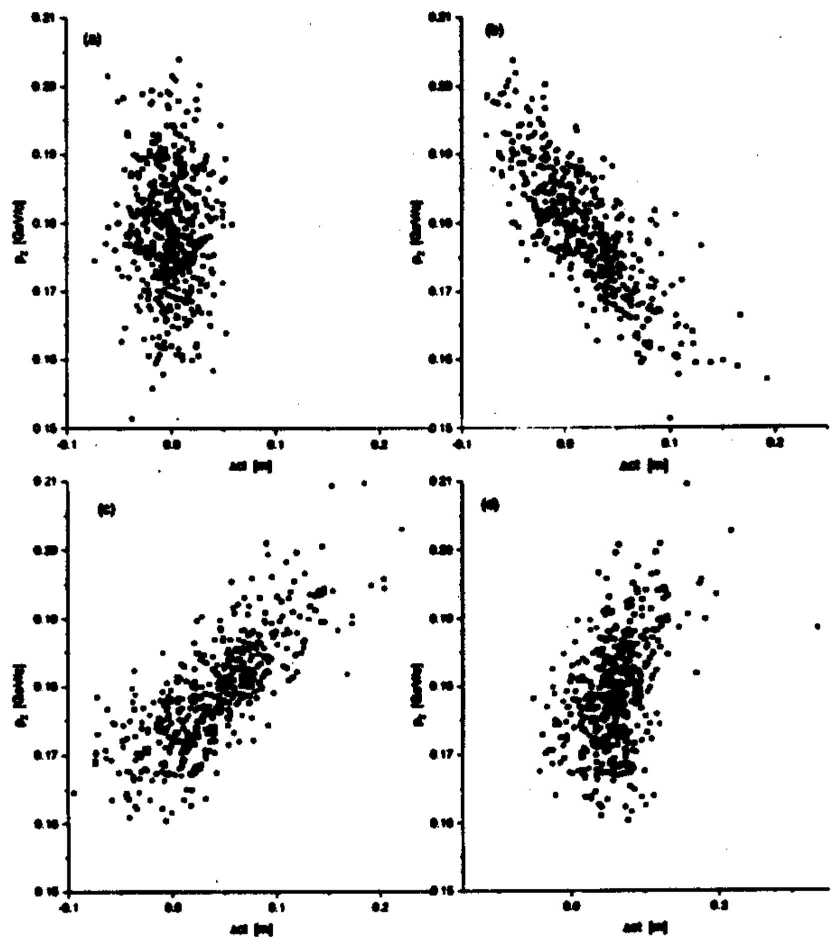

distorted

Figure 8. Longitudinal phase space distribution, p_z *vs* ct (a) at production; (b) after BS1; (c) after RF1; (d) after BS2.

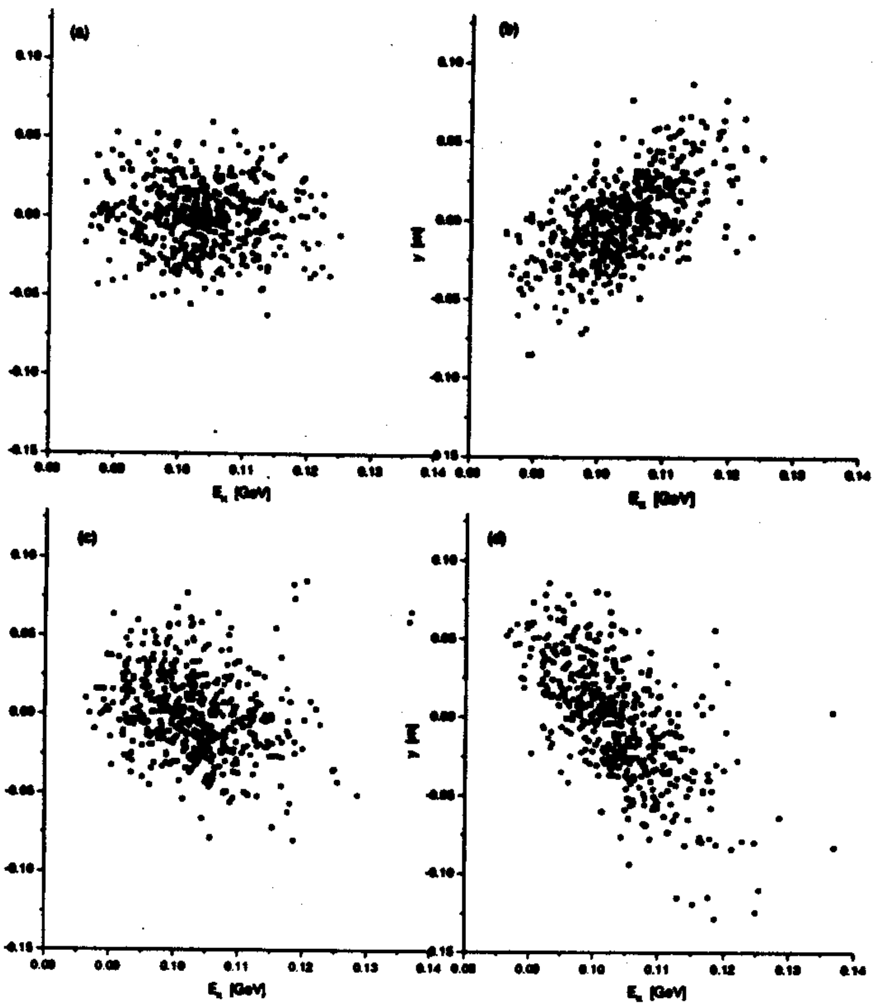

Figure 9. Dispersion distribution, y *vs* E_K (a) at production; (b) after BS1; (c) after RF1; (d) after BS2.

3.2 Wedge design

$$
\begin{aligned}
L_o &= \frac{f\,\Gamma}{n\left\langle \frac{dE}{dz} \right\rangle} \\
w &= 2D\frac{\Gamma}{p_o} \\
h &= \pm 4\sigma_{ND} \qquad\qquad (1) \\
\tan\frac{\alpha}{2} &= \frac{L_o}{w} \\
L_2 &= 2w\tan\frac{\alpha}{2} \le L_{region}
\end{aligned}
$$

where f is the fraction of the momentum spread we want to remove, Γ is the full half-width of the momentum spread, n is the number of thin wedges we are using, $\langle dE/dz \rangle$ is the average energy loss in the wedge material, D is the dispersion, w is the width along the dispersion direction, h is the width in the direction perpendicular to the dispersion, and α is the full vertex angle.

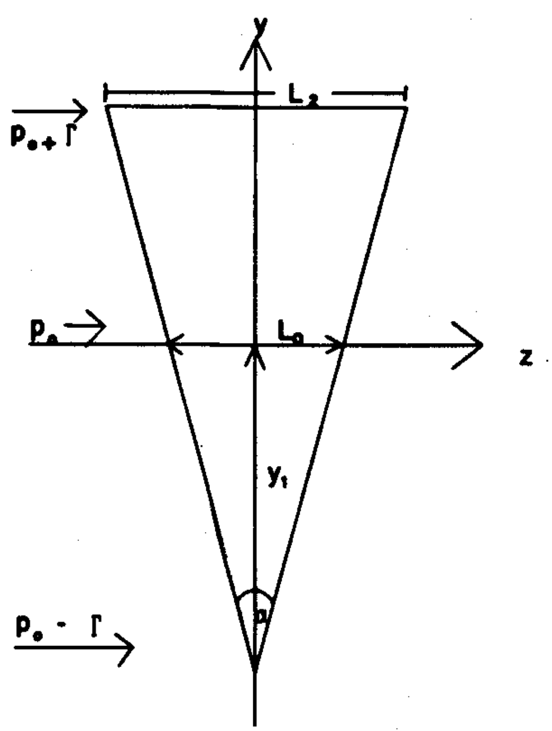

Figure 4. Linear wedge dimensions.

Table 5 Wedge design parameters

material	LiH	
N_{wedges}	4	
L_{region}	27	cm
α	13	deg
φ	90	deg
w	22	cm
h	22	cm

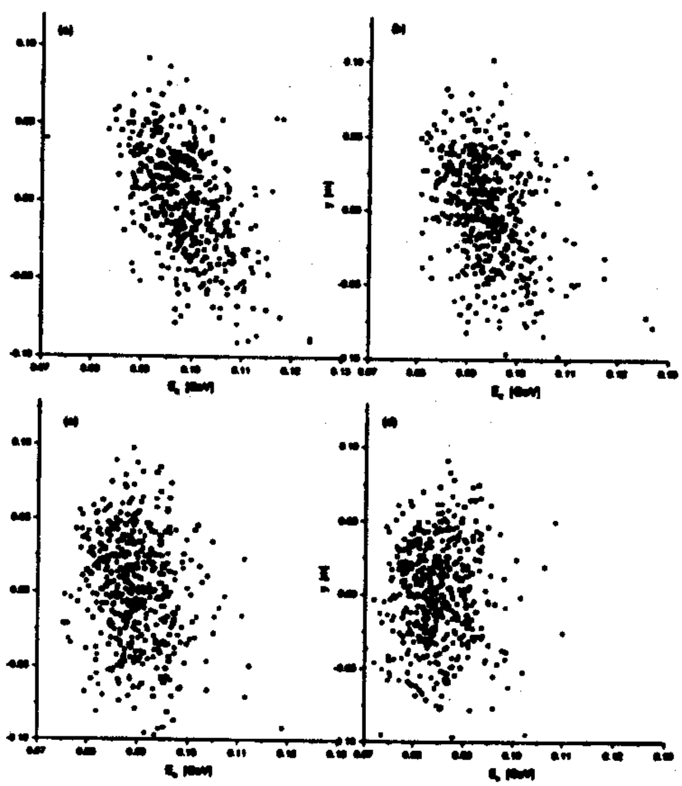

Figure 10. Dispersion distribution, y *vs* E_K (a) after wedge 1; (b) after wedge 2; (c) after wedge 3; (d) after wedge 4.

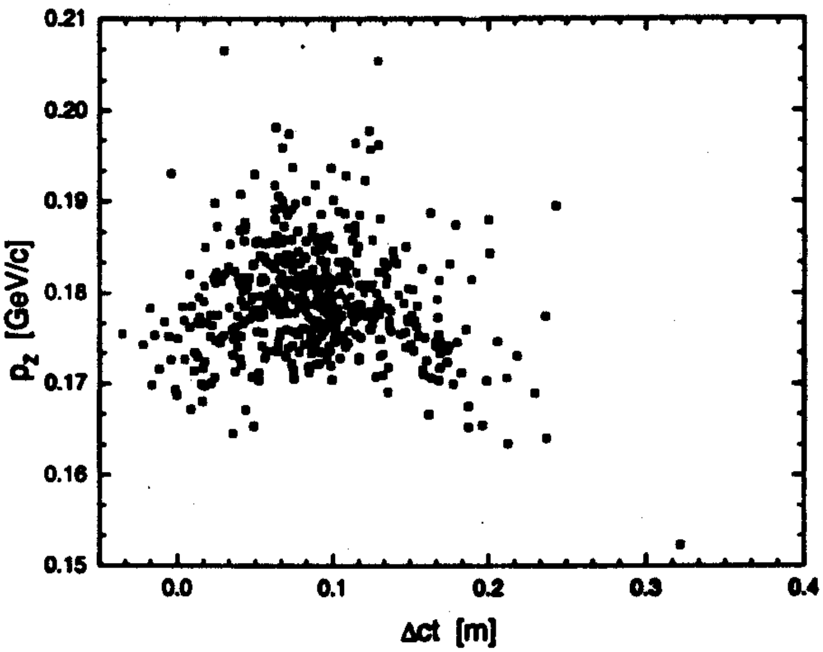

Figure 11. Longitudinal phase space distribution at the end of the (half) emittance exchange system.

Table 2 Beam parameters			
	Entrance	Exit	
p_o	180	180	MeV/c
σ_X	21.1	19.1	mm
σ_Y	21.2	36.4	mm
σ_Z	20	68	mm
σ_{Px}	14.9	13.8	MeV/c
σ_{Py}	15.6	14.2	MeV/c
σ_{PZ}	9.2	7.1	MeV/c
ε_{TN}	2.08	2.79	mm
ε_{LN}	1.68	2.17	mm
ε_{6N}	7.1	14.8	mm^3

Table 6 System performance						
	Start	BS1	RF1	BS2	WED	RF2
<KE> [MeV]	103.2	103.2	103.1	103.1	84.9	103.3
σ_{KE} [MeV]	7.76	7.76	7.83	7.83	6.47	6.44
σ_α [cm]	2.3	4.6	5.7	5.4	5.9	8.1
r (x, KE)	-0.03	0.01	0.02	0.01	0.21	0.19
r (y, KE)	-0.02	0.60	-0.17	-0.65	-0.09	-0.28
r (t, p_Z)	-0.04	-0.80	0.58	0.17	-0.29	-0.44

Conclusions

- no satisfactory solution found yet
- behaves roughly as expected, but no component works ideally
- complicated dynamics between bent solenoids and rf cavities
- error build-up limits performance
- huge parameter space to explore
- theoretical guidance would be helpful